Improving textural properties of γ-alumina by using second generation biomass in conventional hydrothermal method

Cristiane S. Cardoso [1], Yordy F. Licea [2], Xing Huang [3], Marc Willinger [3], Benoit Louis [4,*] and Marcelo M. Pereira [1,*]

[1] *LACES (Laboratório de Catálise e Energia Sustentável) – Instituto de Química da Universidade Federal do Rio de Janeiro, Avenida Athos da Silveira Ramos,149, bloco A, Ilha do Fundão, RJ,CEP:21941-909*

[2] *Instituto de Química da Universidade Federal do Rio de Janeiro, Avenida Athos da Silveira Ramos,149, bloco A, Ilha do Fundão, RJ,CEP:21941-909*

[3] *Department of Inorganic Chemistry, Fritz Haber Institute of the Max Planck Society, Faradayweg 4-6, Berlin 14195, Germany*

[4] *Laboratoire de Synthèse, Réactivité Organiques et Catalyse, Institut de Chimie, UMR CNRS 7177, Université de Strasbourg, 1 rue Blaise Pascal, 67000 Strasbourg Cedex, France*

**Corresponding authors: maciel@iq.ufrj.br; blouis@unistra.fr*

Abstract

The present study reports a simple and inexpensive method for improving the textural properties and stability of γ-alumina by adding crushed sugar cane bagasse to the synthesis gel (highly crystalline bayerite was used as an aluminum source). The influence of bagasse was evaluated by varying the biomass / bayerite ratio from 0.05 to 1 wt%. The presence of bagasse increased both surface area and pore volume up to 2.5-fold and 1.5-fold respectively; yet mesopores with a mean diameter

of 5 nm were observed, which were further increased to 6 nm using hydrolyzed biomass prior to the synthesis. HRTEM measurements highlighted that the presence of biomass raised the formation of pores by enclosure of (111) and (002) lattice planes.

Keywords: alumina, biomass, mesopores, hydrothermal synthesis

1. Introduction

Nowadays more than 90 million tons of alumina is produced per year for several purposes [1]. Particularly γ-alumina is widely used as a support in several petrochemical processes [2] (catalytic cracking, hydrotreatment and hydrogenation reactions), thanks to its high surface area and thermal stability compared with other alumina polymorphs. The improvement of alumina textural properties as well as its thermal stability is of prime importance, *i.e.* raising pore size and volume is accompanied by higher mass transfer, thus leading to a better access toward the catalytic sites. Indeed, the higher the surface area is, the lower mass of catalyst is required in a process. Hence this study is of great interest for both academic and industrial research.

Alumina precursors as boehmite and bayerite are prepared by the conventional hydrothermal routes [3], yielding after a thermal treatment in the range of 500-700^{o}C, γ-alumina which exhibits specific surface areas (BET) up to 200 m^2/g [4]. However, this simple and cheap method does not lead to large pore sizes and volumes [2]. Several strategies have therefore been undertaken to enhance these textural properties in a pre-synthesized colloidal sol-gel system, as for example: organic solvent use [5], addition of structural agents. The latter approach has been largely explored, for instance dual soft templates and co-polymers [5b, 6], surfactants [7], hard templates [8], and besides, a combination of a dual soft template resulted in alumina containing

macro- and mesopores in the range of 100-600 nm and 8-10nm, respectively [9]. By a proper control of water content in aluminum alkoxide precursors, without assistance of structural agents, γ-alumina with a high surface area and large pore size with broad dispersion was recently produced by Bartholomew *et al.* [10]. Though, our intention is not to extensively describe these methods, textural properties of some γ-alumina obtained in the literature are presented in Table 1. However, it is important to point out that these methods remain quite sophisticated and expensive with respect to conventional hydrothermal route. The applicability may therefore be hindered in domains involving loss of material or deactivation like in fluid catalytic cracking process [11]. As an alternative to these sophisticated methods, alumina with BET area comprised between 230-315 m^2/g and pore diameter in the range of 3-4 nm were prepared in the presence of methyl-cellulose [12]. Yeast cells were also used for preparing alumina [13], resulting in macro- and mesopores in the range of 1.5-3 μm and 3-4 nm, respectively. Likewise, specific surface areas up to 343 m^2g^{-1} were achieved. Finally, sugars and polysaccharides largely improved alumina areas (Table 1) but at the expense of crystallinity [14].

γ-alumina structure is often described by a defect cubic spinel structure exhibiting Fm-3m space group (ICSD number 030267) [10]. Furthermore, γ-alumina is typically formed via topotatic transformation of boehmite [15]. The stacking of γ-alumina matrix could be related to oxygen sub-lattice from boehmite. The arrangement of crystallites into corresponding boehmite determines γ-alumina morphology and porosity due to the pseudomorphic transformation of one phase into another [16]. Transitions alumina (up to α-alumina) undergo meta-stable transformations [17] in both crystal self-assembly processes during pre-synthesized colloidal sol-gel system and during thermal treatment. These steps involved in the precursor transformation to γ-alumina could be affected by the presence of organic molecules according to a supramolecular mechanism.

Sugar cane bagasse, a second generation biomass, is a by-product of sugar and ethanol production in Brazil for example [18]. The introduction of biomass residues was already performed in the synthesis of zeolites [19], leading to smaller crystal size in the range of 50-100 nm, but none report focusing on alumina preparation could be found using these agricultural crops. Herein, γ-alumina was prepared by a conventional hydrothermal method in the presence of sugar cane bagasse. Highly crystalline bayerite was used as an aluminum source and the relative amount of biomass regarding bayerite was varied from 1 to 0.05 (in wt%) and yet alumina was prepared in the presence of modified biomass by prior hydrolysis.

2. Experimental Section

2.1 Materials

Bayerite alumina, $Al(OH)_3$, with the following composition in wt%: 64.2 Al_2O_3, 0.03 K_2O, 0.04 CaO, 0.02 CuO, 0.04 Fe_2O_3, 0.05 SiO_2, 0.01 ZnO, 35.61 H_2O was used as an aluminum source. The sugar cane bagasse (cellulose 40.0 %, hemicellulose 33.4%, lignin 7.1% *in weight*) was dried at room temperature, crushed and sieved in 20-80 mesh particles. All reagents were used without further purification.

2.2 Alumina preparation

Two references alumina (without biomass introduction) were synthesized. Firstly, 2 g of bayerite was added to 5 mL of deionized water (obtained by Simplicity UV–Millipore equipment) at room temperature. These components were mixed during 10 min using a mortar and pestle, then transferred to an autoclave and kept for 16 h at 423 K under autogeneous pressure. The resulting white gel was subsequently filtered and washed with deionized water, calcined in a muffle furnace in air at 600ºC for 2h (at a heating rate of 10ºC/min). This alumina was named

Al_2O_3REF1. Besides, a second alumina labeled Al_2O_3REF2 was obtained through straight thermal treatment of bayerite in air at 600ºC during 2h (10ºC/min heating rate).

Alumina was prepared in the presence of sugar cane bagasse "*in natura*" using various biomass / bayerite ratios: 1:1, 1:5, 1:10, 1:15 and 1:20. The same sol-gel preparation for Al_2O_3REF1 was performed with different amounts of biomass added to 2 g of bayerite to reach aforementioned quantities. Likewise, the thermal treatment was the one chosen for Al_2O_3REF1. As-prepared aluminas in the presence of biomass residues were named according to biomass / bayerite ratios: Al_2O_3BM1:1, Al_2O_3BM1:5 and so on. Besides the alumina prepared, using the sugar cane fibers in the proportion 1:10, another alumina was synthesized using the alkaline hydrolysis solution without sugar cane fibers. Pristine sugar cane residues were hydrolyzed in a NaOH (0,5M) aqueous solution in a flat-bottomed flask for 1h at 130ºC. The pH was set to 12 to guarantee the same conditions of alumina preparation. The residual bagasse was filtered and washed with deionized water and thermally treated in a muffle furnace in air overnight at 100°C. 0.2 g of this sample, labeled Al_2O_3SBM 1:10, was used. In the preparation of alumina with hydrolyzed sugar cane bagasse, 2 g of bayerite was mixed with 4 mL of hydrolyzed biomass solution at room temperature. This sample was named Al_2O_3HBM.

2.3 Characterization

Nitrogen adsorption-desorption measurements were carried out using a ASAP 2010 Micromeritics volumetric apparatus. Prior to the measurements, the samples were outgassed in vacuum at 300ºC overnight. Specific surface areas (SSA) were calculated according to the Brunauer-Emmett-Teller (BET) method, using a P/P_0 range between 0.05 and 0.2. Pore volumes (PV) were determined by the BJH method from the isotherm adsorption branch.

X-ray Diffraction (XRD) was performed using a Rigaku Ultima IV diffractometer (Cu $_{K\alpha}$ λ = 0.1542 nm) at a scanning rate of 0.02 ° s^{-1} in 2θ ranges from 5 to 80°. A fixed power source was used (40kV, 20 mA). All alumina precursors were dried at 100°C overnight before the measurements. XRD peaks corresponding to (111) and (222) planes were fitted using Gaussian functions to have a qualitative information weighted by the eta or gamma alumina characteristics of the pattern profile. The shape factor was assumed to unity by considering spherical particles.

The n-hexane adsorption was performed in a TG 209 F1 Iris Netzsch thermal analyzer in alumina crucibles (85µL). The sample was pre-treated at 600ºC for 30 min in a N_2 flow of 30 mL/min. The temperature was then lowered to 40°C in N_2 atmosphere and maintained during 30 min. A 60 mL/min flow consisting of 7.2 v/v% of n-hexane in N_2 at ambient pressure was flown through the sample during 30 min. Thermogravimetric analysis (TGA) was performed using a NETZSCH STA449F1 instrument. For these experiments, 10 mg of dried precursor was heated from 50°C to 700°C in the presence of helium and subsequently heated to 1000 °C (10°C/ min in a 5% O_2/He atmosphere).

^{27}Al MAS NMR spectra recorded at 1500 Hz were acquired on a Bruker Avance 400 (9.4 T) spectrometer. The number of accumulations was set to 1024 along with a sequence of polarization at pulse intervals of 0.5 s. A sample of $[Al(H2O)_6]^{3+}$ was used as external reference (0.0 ppm).

Transmission electron microscopy (TEM) and high-resolution TEM (HRTEM) images, as well as selected area electron diffraction (SAED) patterns of the materials were recorded using an FEI aberration-corrected Titan 80-300 microscope operated at 300 kV.

3. Results

γ-alumina prepared by conventional hydrothermal method using highly crystalline boehmite or bayerite usually exhibits SSA in the range of 40-120 m^2/g and

pore volume of approximately 0.3 cm^3/g [13], or SSA up to 200 m^2g^{-1} with pore diameter lower than 3 nm [4]. In contrast, sophisticated methods usually yield alumina with improved or tailored textural properties (Table 1).

After performing the hydrothermal syntheses, all alumina were thermally treated at 600°C to remove all organics. After thermal treatment, the amount of released water was nearly identical in all alumina, 3 wt.% up to 200°C and 3 wt.% between 200°C and 700°C (Figure not shown). Table 2 summarizes the textural properties of both references and sugar cane-mediated aluminas. Al_2O_3REF1 and Al_2O_3REF2 samples exhibit similar textural properties. In contrast, all as-synthesized alumina in the presence of pristine bagasse, regardless its quantity, exhibit higher SSA and pore volumes when compared with reference aluminas. For instance, Al_2O_3BM1:10 sample showed a 2.5-fold and a 1.5 fold increase in BET area with respect to REF 1 and REF2, respectively. This remarkable result confirms the possibility to modify alumina textural properties by adding biomass residues in the hydrothermal step of alumina preparation. Furthermore, it is important to point out that SSA was slightly affected by the amount of bagasse, with an apparent maximum for Al_2O_3BM1:10. However, alumina prepared in the presence of sugar cane bagasse previously submitted to an alkaline treatment, Al_2O_3SBM1:10, led to a lower BET area compared with Al_2O_3BM1:10 sample but to larger porous diameter. The latter alkaline treatment removes preferentially lignin components and partly hemicellulose[20]. These results suggest that the type of biomass in relation to its composition and / or topology could be an important parameter in the design of tailor-made alumina. In contrast to the presence of biomass itself, the synthesis of alumina performed in the presence of alkaline biomass hydrolysis solution neither increased the BET area nor the pore volume. These properties remained similar to those of Al_2O_3REF1.

The amount of n-hexane adsorbed on each alumina is plotted against the SSA values (Figure 1). The alkane adsorption was increased while raising the SSA of

alumina prepared with sugar cane residues; this is in agreement with the data related to textural properties (Table 2). Surprisingly, BET areas were rather similar for 1:1 to 1:10 bayerite / bagasse ratio whilst a nearly 30% higher hexane quantity was adsorbed on Al_2O_3BM1:10 with respect to Al_2O_3BM1:1 sample. The presence of a primary microporous structure and connected pores (also supported by nitrogen adsorption-desorption isotherms and HRTEM images in coming sections) may partially explain these results.

The adsorption-desorption isotherms and distribution of pores are presented in Figures 2 and 3, respectively. All alumina prepared by hydrothermal method exhibited a type IV isotherm, thus confirming the presence of mesopores [10]. The presence of H2-type and H4-type hysteresis, according to IUPAC classification [21] can be observed for the two references alumina (Figure 2a). However, Al_2O_3REF2 exhibits a rather different pore organization with higher interconnectivity compared with Al_2O_3REF1. Hysteresis phenomenon is related to both adsorption-desorption and porous network connectivity and the presence of such hysteresis type indicates a rather complex porous structure with minor ordering when compared with other crystalline materials [22].

Figure 2b shows the isotherms for Al_2O_3 BM1:10, Al_2O_3SBM1:10 and Al_2O_3HBM (alumina prepared in the hydrolyzed solution of biomass). It seems that an ordering is gained in porous network ranging from the later to the former two materials. Likewise, Al_2O_3 BM1:5 and Al_2O_3 BM1:1 isotherms (Figure 2c) further support pore ordering, exhibiting a H2-type adsorption hysteresis being a consequence of pore interconnectivity [23]. The presence of a sharp adsorption step in the P/P_0 region between 0.4 and 0.6 in the hysteresis loop supports the existence of a well-defined array of regular mesopores (Figures 2b). Regarding pore sizes (Figure 3), a regular and narrow distribution of mesopores with mean diameter size around 5 nm was formed over bagasse-templated aluminas. In contrast, a broad distribution of larger mesopores (3-12 nm) was observed for Al_2O_3REF2 material (Figure 3a).

Though all these alumina contain mesopores, it can also be extracted from these data, that Al_2O_3REF2 and Al_2O_3-mediated bagasse samples (BM 1:10 mainly) possess rather different pore organization with higher interconnectivity for the later materials.

XRD diffraction patterns of all alumina after hydrothermal synthesis followed by thermal treatment at 600°C are presented in Figure 4. *Eta* and *gamma* alumina were obtained by thermal treatment of bayerite and boehmite, respectively [4]. It is noteworthy that bayerite was converted into boehmite upon dehydration.

Table 2 presents the values of coherent domain lengths determined by the Scherrer formula from the FWHM Gaussian function fitted for the profiles in [111] and [222] planes, as well as the ratio between these two diameters.

Al_2O_3REF1 and Al_2O_3REF2 samples showed a large difference in this ratio, being 0.15 and 1.03, respectively. This ratio increased from 0.4 in Al_2O_3BM1:1 to 0.7 in Al_2O_3BM1:10. Likewise, the distance of (111) coherent domain was largely increased while introducing biomass residues, from 21 Å in REF1 alumina up to 114 Å in Al_2O_3BM1:10 sample. It is important to point out that polycrystal X-ray is an average of many crystals, and yet, mixtures of *eta* and *gamma* alumina phases could take place. A precise resolution of alumina structure cannot be provided by the sole XRD technique [17a].

Both L(A)(111) / L(A)(222) ratio and BET area were normalized and plotted against the amount of biomass (Figure 5). Whereas the tendency in BET area is to increase with biomass percentage and then to level off, in contrast the crystal L(A)(111)/L(A)(222) ratio diminished. It seems therefore to be a correlation between these two normalized values, suggesting an optimum weight percentage of biomass needed to improve the alumina textural properties.

Based on these aforementioned data (Table 2 and Figure 1), it appears that the presence of bagasse itself in the hydrothermal step is responsible for enhancing the

alumina textural properties. Hence the type and nature of biomass residues seem to affect the process of alumina crystals self-assembly.

Figure 4a shows that bayerite underwent phase transition to boehmite in REF1 alumina, yielding after thermal treatment γ-alumina phase formation. Figure 4b presents the pattern of REF2 alumina formed after direct thermal treatment of bayerite. When biomass was introduced in the preparation gel, the transition of bayerite to boehmite was partially hindered, as for instance in Al_2O_3BM 1:1 sample (Figure S1). Al_2O_3BM 1:10 also exhibits diffraction patterns of boehmite, but in a lower amount compared with Al_2O_3BM 1:1. The amount of boehmite in former alumina was not determined since (020) reflection is absent; smaller crystal size or highly oriented crystals could explain this observation. However, it is important to point out that hindering bayerite dehydration cannot be related to the amount of water consumed during the hydrolysis of biomass components, like for example in the preparation of Al_2O_3BM 1:10. The water amount present in the reaction is two orders of magnitude higher than the amount necessary for hydrolyzing the whole cellulose (1,4-glycoside bond) and hemi-cellulose present in sugar cane bagasse. As a consequence the hampering of bayerite / boehmite phase transition observed for Al_2O_3BM 1:10 could be mainly related to organic compounds formed *in-situ* or *to* biomass itself interacting with gel particles.

To summarize this part, the use of sugar cane bagasse as sacrificial template led to major modifications in the organization of alumina phase, both in terms of porosity as well as long distance ordering. To further confirm these observations, HRTEM measurements were performed over Al_2O_3REF1 and Al_2O_3BM1:10 aluminas (Figure 6). As shown in Figure 6b and d, both samples demonstrated regular alumina planes. Al_2O_3REF1 is formed by oriented lamellar structure, which assemble into a compact ‘‘card-pack’’ microstructure upon annealing (Figure 6a). In contrast, Al_2O_3 BM1:10 exhibited a regular porous distribution in the lamellar structure (Figure 6d). Yet these pores showed diameter with wide dispersion from 1 to 8 nm, being mainly

centered around 2-4 nm (Figure 7). HRTEM results indicate that these pores are mainly formed by enclosure of alumina (111) and (002) planes. Pore size distribution in the range of 3.5-15 nm was observed when alumina was prepared in the presence of non-ionic surfactants [7].

Aluminum distribution determined by ^{27}Al MAS NMR (Figure S2) for both Al_2O_3 REF1 and Al_2O_3 1:10BM show identical Al (IV) and Al (VI) amounts in line with literature [24]. This result suggests that biomass derived compounds did not affect the bulk alumina, but rather acted locally in the topotatic transformation according to the aforementioned results on textural properties. One may therefore suppose a peculiar interaction during the hydrothermal synthesis between alumina precursor and biomass compounds being responsible for the formation of these ordered pores. The presence of biomass fibers or compounds produced under *in situ* conditions, affects the hydrothermal transition from bayerite to boehmite but this cannot explain the effect on alumina properties since Al_2O_3REF2 is rather different from the one prepared in the presence of biomass. It seems reasonable that during the hydrothermal synthesis some planes could be blocked by biomass compounds produced under *in situ* conditions, which in turn affects the self-assembly process, resulting in a complex connectivity of pores. This could be the reason why n-hexane adsorption did not follow the same trend as pore volume and BET values for biomass-mediated aluminas.

The mechanisms involved for explaining the effect on alumina textural properties assisted by organic compounds are rather scarce in the literature [25]. They include H-bond interactions between large surfactants and AlO(OH) surface which allows the boehmite crystallites to grow along one direction [25a]. The agglomeration of boehmite into structures containing boehmite and sandwich-type co-polymers led to the formation of larger pseudo-boehmite nanoparticles in solution. Menu *et al.* [5b] have recently shown that ethylene co-polymer favors particles alignment, which after

annealing creates the porous network where micelles can act as space fillers, hence generating large pores, up to 14 nm [5b].

4. Tentative growth mechanism

In terms of mechanism understanding, our results can be related to the presence of large biomass-derived compounds, such as polysaccharides or large phenolic compounds and / or alternatively to numerous molecules that play a central role in the self-assembly process in alumina crystals formation. However, the pore formation is not the result of gel particle formation around biomass residues [13]. Neither textural properties nor XRD patterns were affected when alumina was prepared in the presence of an alkaline hydrolyzate solution of biomass fibers under the same conditions of reference alumina preparation. One cannot rule out the possibility of these species being largely different from those formed during alumina preparation in the presence of biomass. In addition, the improvement of alumina textural properties was not largely affected by biomass quantity, but rather by the type of biomass (when biomass was previously hydrolyzed). One can therefore argue that under *in situ* conditions, hydrolyzed polysaccharides may be the key components in modifying alumina textural properties. Further studies are under progress to get a deeper understanding on the nature of the organic compounds, formed in solution, being responsible for peculiar crystal growth in those biomass-mediated materials.

The latter molecules, related to biomass composition, are probably interacting with hydroxyl groups in the gel precursor. This phenomenon may result in a partial blocking of both bayerite dehydration to boehmite and crystal connectivity, which in turn is responsible for generating a highly ordered porous structure (HRTEM results). Indeed, it was proposed that monosaccharides interacted strongly with gel particles[14]. It was also shown that xylitol preferentially interacts with boehmite lateral

faces rather than basal faces [26], hence creating an interaction with boehmite via hydrogen bonds. The preferential interaction with non-basal faces perfectly agrees with HRTEM measurements, where the number of lateral faces increased when alumina was prepared in the presence of biomass. Finally, it should also favor the self-assembly of hundreds of nanometer-sized crystals, as suggested by XRD data.

In terms of improving alumina textural properties, our results are rather promising compared with those found in literature. Nevertheless, higher textural properties (larger and narrow mesopores, good thermal stability) can be generally achieved using more sophisticated methods. However, the results reported herein put on alert that these cheap crop residues could be valorized, resulting not only in improving the catalyst support properties but also in mitigating environmental damage.

5. Conclusion

Alumina was successfully prepared in the presence of biomass residues (sugar cane bagasse) using conventional hydrothermal route and highly crystalline bayerite precursor. The presence of bagasse raised the specific surface area, pore volume and mesopores (with mean diameter of 2-4 nm). These mesopores were produced by enclosure of (111) and (002) lattice planes.

Moreover, the presence of biomass (the nature rather than its amount) strongly affected the self-assembly process of the crystals.

References

1. Institute, I. A. Statistic on alumina production, http://www.world-aluminium.org/statistics/alumina-production/ - histogram, 2014.
2. Márquez-Alvarez, C.; Zilková, N.; Pérez-Pariente, J.; Jiri, C. *Catal. Rev. Sci. Eng.* **2008,** *50*, 222-286.
3. (a) Mishra, D.; Anand, S.; Panda, R. K.; Das, R. P. *Mater. Lett.* **2000,** *42*, 38–45; (b) Somiya, S.; Roy, R. *Bull. Mater. Sci.* **2000,** *23*, 453–460.

4. Maciver, D. S.; Tobin, H. H.; Barth, R. T. *J. Catal.* **1963,** *2*, 485-497.
5. (a) Gan, Z.; Ning, G.; Lin, Y.; Cong, Y. *Mater. Lett.* **2007,** *61*, 3758-3761; (b) Bleta, R.; Alphonse, P.; Pin, L.; Gressier, M.; Menu, M. J. *J Coll. Inter. Sci.* **2012,** *367*, 120-128.
6. Sun, L. B.; Yang, J.; Kou, J. H.; Gu, F. N.; Chun, Y.; Wang, Y.; Zhu, J. H.; Zou, Z. G. *Angew. Chem. Int. Ed. Engl.* **2008,** *47*, 3418-3421.
7. Zhang, Z.; Pinnavaia, T. J. *Langmuir* **2010,** *26*, 10063-10067.
8. Wu, Z.; Li, Q.; Feng, D.; Webley, P. A.; Zhao, D. *J. Am. Chem. Soc.* **2010,** *132*, 12042-12050.
9. Martins, L.; Alves Rosa, M. A.; Pulcinelli, S. H.; Santilli, C. V. *Microporous Mesoporous Mater.* **2010,** *132*, 268-275.
10. Huang, B.; Bartholomew, C. H.; Woodfield, B. F. *Microporous Mesoporous Mater.* **2014,** *183*, 37-47.
11. O'Connor, P., Catalytic cracking: The Future of an Evolving Process. *in Stud. Surf. Sci. Catal.*, Ocelli, M. L., Ed. Elsevier: 2007; Vol. 166, pp 227-251.
12. Zhong, L.; Zhang, Y.; Chen, F.; Zhang, Y. *Microporous Mesoporous Mater.* **2011,** *142*, 740-744.
13. Ma, Y.; Wei, Q.; Ling, R.; An, F.; Mu, G.; Huang, Y. *Microporous Mesoporous Mater.* **2013,** *165*, 177-184.
14. Xu, B.; Long, J.; Tian, H.; Zhu, Y.; Sun, X. *Catal. Today* **2009,** *147*, S46-S50.
15. Paglia, G.; Buckley, C. E.; Udovic, T. J.; Rohl, A. L.; Jones, F.; Maitland, C. F.; Connolly, J. *Chem. Mater.* **2004,** *16*, 1914-1923.
16. Sanchez-Valente, J. S.; Bokhimi, X.; Hernandez, F. *Langmuir* **2003,** *19*, 3583-3588.
17. (a) Levin, I.; Brandon, D. *J. Am. Ceram. Soc.* **1998,** *81*, 1995–2012; (b) Santosa, P. S.; Santos, H. S.; Toledo, S. P. *Mater. Res.* **2000,** *3*, 104-114.
18. Hofsetz, K.; Silva, M. A. *Biomass & Bioenergy* **2012,** *46*, 564-573.
19. Ocampo, F.; Cunha, J. A.; de Lima Santos, M. R.; Tessonnier, J. P.; Pereira, M. M.; Louis, B. *Appl. Catal. A* **2010,** *390*, 102-109.
20. Cunha, J. A.; Pereira, M. M.; Valente, L. M. M.; de la Piscina, P. R.; Homs, N.; Santos, M. R. L. *Biomass and Bioenergy* **2011,** *35*, 2106-2116.
21. Sing, K. S. W.; Everett, D. H. ; Haul, R. A. W.; Moscou, L.; Pierotti, R. A.; Rouquerol, J.; Siemieniewska, T. *Pure & Appl. Chem.* **1985,** *57*, 603-619.
22. Naumov, S. Hysteresis Phenomena in Mesoporous Materials. PhD Thesis, Leipzig University, 2009.
23. Mason, G. *J. Coll. Inter. Sci.* **1981,** *88*, 36-46.
24. Samain, L.; Jaworski, A.; Edén, M.; Ladd, D. M.; Seo, D. K.; Javier Garcia-Garcia, F.; Häussermann, U., *J. Solid State Chem.* **2014,** *217*, 1-8.
25. (a) Zhu, H. Y.; Riches, J. D.; Barry, J. C., *Chem. Mater* **2002,** *14*, 2086-2093; (b) Fulvio, P. F.; Brosey, R. I.; Jaroniec, M., *ACS Appl. Mater. Inter.* **2010,** *2*, 588-593.
26. Chiche, D.; Chizallet, C.; Durupthy, O.; Chaneac, C.; Revel, R.; Raybaud, P.; Jolivet, J. P. *Phys. Chem. Chem. Phys.* **2009,** *11*, 11310-11323.

Figure captions

Table 1. Textural properties of alumina (BET area, pore volume and pore diameter)

Table 2. Textural properties: specific surface area, pore volume, crystallite size and full-width at half-maximum (FWHM) for (111) and (222) planes for all materials.

Figure 1. n-hexane adsorption versus BET area for Al_2O_3REF1 alumina and aluminas prepared in the presence of biomass Al_2O_3 BM1:1, Al_2O_3 BM1:5, Al_2O_3 BM1:10.

Figure 2. Nitrogen adsorption-desorption isotherms of (a) Al_2O_3REF1 and Al_2O_3REF2 (b) Al_2O_3 BM1:10, alumina prepared with fiber residual hydrolysis treatment (Al_2O_3SBM1:10) and alumina prepared in hydrolyzed solution of biomass (Al_2O_3HBM) and (c) Al_2O_3 BM1:1 and Al_2O_3 BM1:5.

Figure 3. Radius distribution in function of dV/dR by BJH method for (a) Al_2O_3REF1 and Al_2O_3REF2 (b) Al_2O_3 BM1:10, alumina prepared with fiber residual hydrolysis treatment (Al_2O_3SBM1:10) and alumina prepared in hydrolyzed solution of biomass (Al_2O_3HBM) and (c) Al_2O_3 BM1:1 and Al_2O_3 BM1:5.

Figure 4. X-ray diffraction patterns (intensity in counts per seconds, CPS) before and after thermal treatment at 600°C for (a) Al_2O_3REF1, (b) Al_2O_3REF2, (c) Al_2O_3 BM1:10, (d) Al_2O_3 BM1:5, (e) Al_2O_3 BM1:1, (f) Al_2O_3 SBM1:10 and (g) Al_2O_3 HBM.

Figure 5. Normalized BET surface area (⌂) and L(111)/L(222) (■) vs biomass weight percentage.

Figure 6. HRTEM images of Al_2O_3REF1 (a,b) and Al_2O_3BM1:10 aluminas (c,d).

Figure 7. HRTEM image of the a) Al_2O_3 BM1:10 and b) respective distribution of diameter size of porous from HR-TEM.

Table 1. Textural properties of alumina (BET area, pore volume and pore diameter)

Type of addition	Al source	BET [m^2/g]	Vol_p [cm^3/g]	D [nm]	Ref
None	Nitrate	80-144	0.11-0.13	3	[13]
Control water amount	Butoxide	300	1.63	7-30	[10]
Control water amount	Boehmite	238	0.3	3-5	[7]
Control water amount	Butoxide	300	0.31	5	[5b]
in toluene/isopropanol	Isopropoxide	365	0.84	1-12	[5a]
Triblock copolymer (2)*	Butoxide	450	1.49	8-16	[5b]
Hard template carbon	Nitrate	261	0.45	4-9	[8]
Surfactant (0.6)*	Boehmite	320	0.7	2-10	[7]
Surfactant (2)*	Boehmite	301	1.1	4-23	[7]
Yest cell	Nitrate	343	0.28	3-4	[13]
Sucrose/Alumina 1:1	Propoxide	464	0.61	2-5	[14]
Cyclodextrin/Al 1:7	Propoxide	260	0.66	3-11	[14]

* Relative amount of organics with respect to aluminum.

Table 2. Textural properties: specific surface area, pore volume, crystallite size and full-width at half-maximum (FWHM) for (111) and (222) planes for all materials.

Sample	m^2/g	cm^3/g	Mean Diam. (nm)	hkl (111) L/(Å)	hkl (111) FWHM	hkl (222) L/(Å)	hkl (222) FWHM	(111)/(222) ratio
Al_2O_3REF1	82	0.22	6.8	21	4.25	167	0.56	0.15
Al_2O_3REF2	144	0.34	7.9	94	0.95	104	0.90	1.03
Al_2O_3BM1:1	198	0.44	7.2	57	1.58	130	0.72	0.4
Al_2O_3BM1:5	207	0.36	5.2	93	0.96	116	0.81	1.04
Al_2O_3BM1:10	209	0.36	5.6	72	1.25	113	0.83	0.69
Al_2O_3SBM1:10	156	0.37	7.8	114	0.79	130	0.73	0.88
Al_2O_3BM1:15	195	0.31	6.0	68	1.31	119	0.79	0.89
Al_2O_3BM1:20	200	0.31	5.8	98	0.91	130	0.72	1.17
Al_2O_3HBM	86	0.25	7.4	15	5.98	184	0.51	0.1

Figure 1. n-hexane adsorption versus BET area for Al_2O_3REF1 alumina and aluminas prepared in the presence of biomass Al_2O_3 BM1:1, Al_2O_3 BM1:5, Al_2O_3 BM1:10.

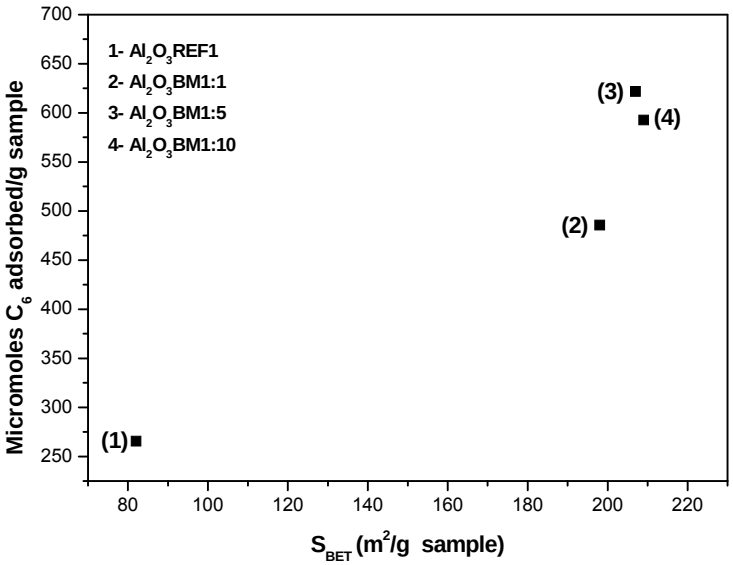

Figure 2. Nitrogen adsorption-desorption isotherms of (a) Al_2O_3REF1 and Al_2O_3REF2 (b) Al_2O_3 BM1:10, alumina prepared with fiber residual hydrolysis treatment (Al_2O_3SBM1:10) and alumina prepared in hydrolyzed solution of biomass (Al_2O_3HBM) and (c) Al_2O_3 BM1:1 and Al_2O_3 BM1:5.

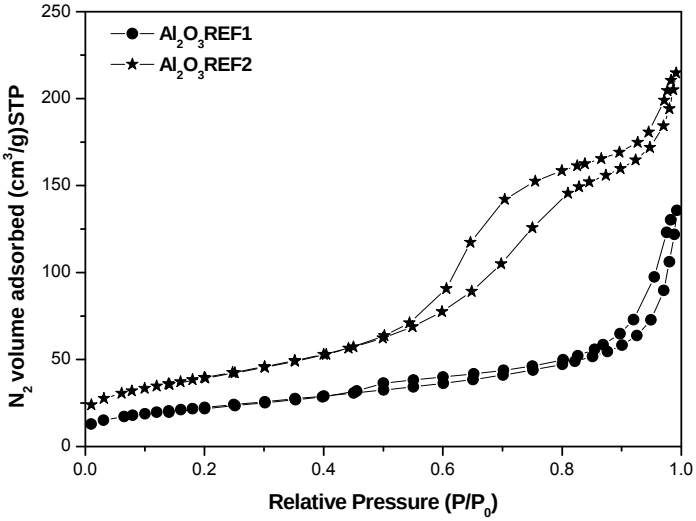

Figure 2a

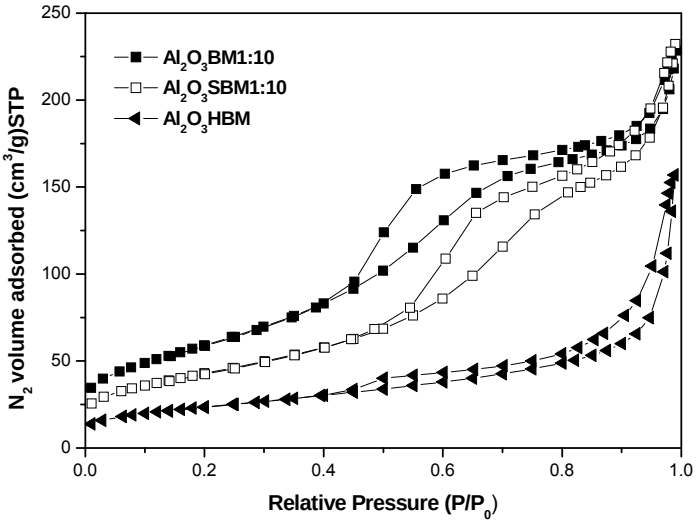

Figure 2-b

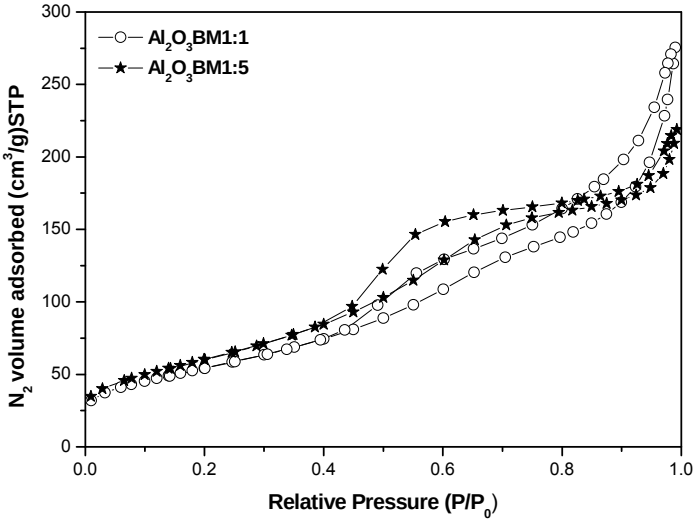
Al2O3BM1:1
Al2O3BM1:5
N2 volume adsorbed (cm3/g)STP
Relative Pressure (P/P0)
0
50
100
150
200
250
300
0.0
0.2
0.4
0.6
0.8
1.0

Figure 2-c

Figure 3. Radius distribution in function of dV/dR by BJH method for (a) Al_2O_3REF1 and Al_2O_3REF2 (b) Al_2O_3 BM1:10, alumina prepared with fiber residual hydrolysis treatment (Al_2O_3SBM1:10) and alumina prepared in hydrolyzed solution of biomass (Al_2O_3HBM) and (c) Al_2O_3 BM1:1 and Al_2O_3 BM1:5.

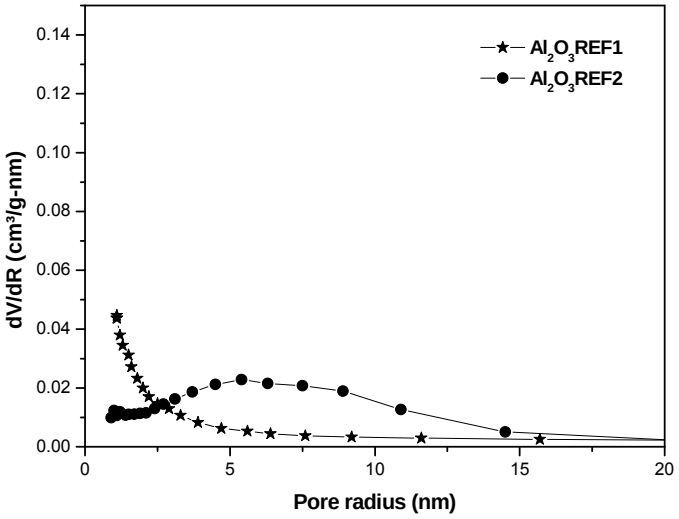

Figure 3-a

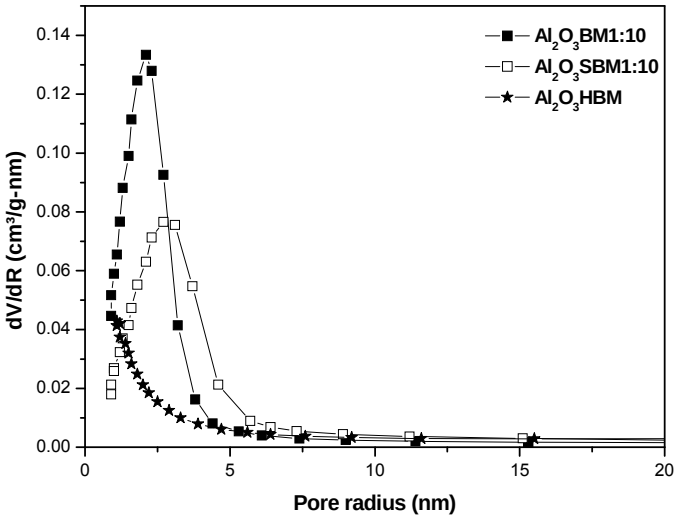

Figure 3-b

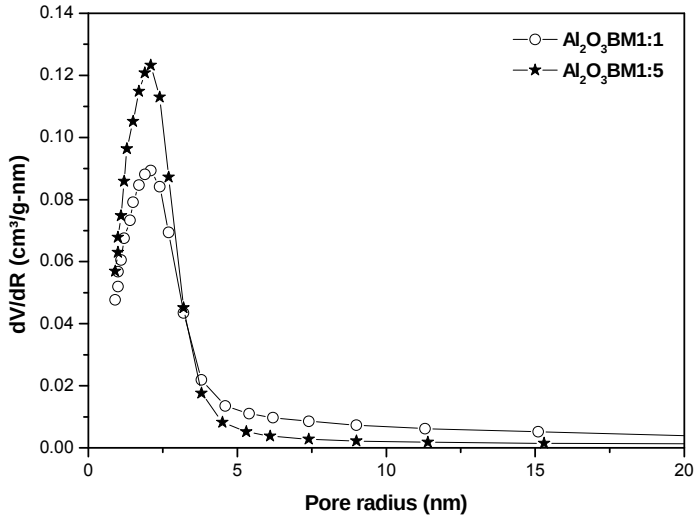
0.14
0.12
0.10
0.08
0.06
0.04
0.02
0.00
dV/dR (cm³/g-nm)
0
5
10
15
20
Pore radius (nm)
Al2O3BM1:1
Al2O3BM1:5

Figure 3-c

Figure 4. X-ray diffraction patterns (intensity in counts per seconds, CPS) before and after thermal treatment at 600°C for (a) Al_2O_3REF1, (b) Al_2O_3REF2, (c) Al_2O_3 BM1:10, (d) Al_2O_3 BM1:5, (e) Al_2O_3 BM1:1, (f) Al_2O_3 SBM1:10 and (g) Al_2O_3 HBM.

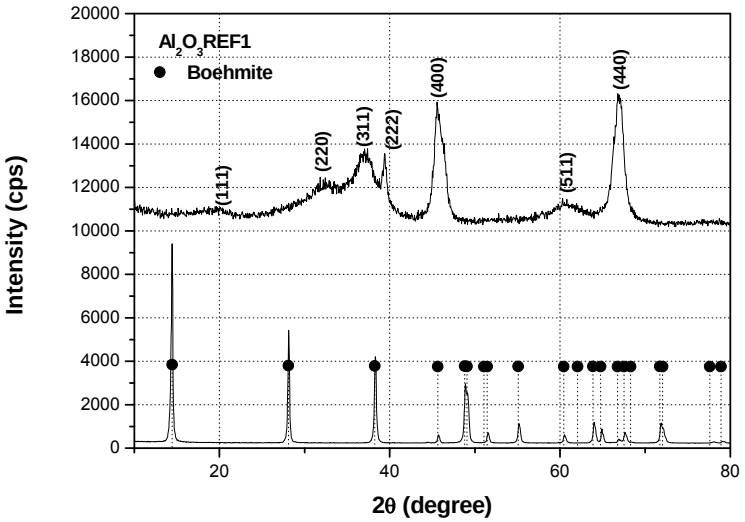

Figure 4-a

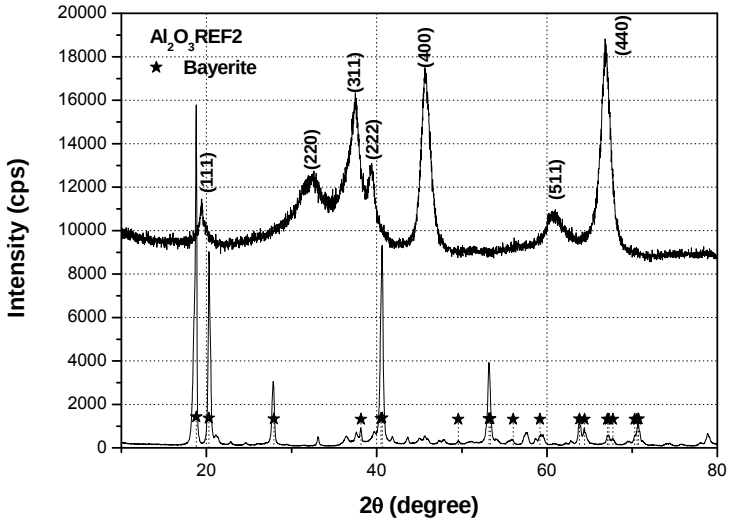
Al2O3REF2
Bayerite
(111)
(220)
(311)
(222)
(400)
(511)
(440)
Intensity (cps)
2θ (degree)
0
2000
4000
6000
8000
10000
12000
14000
16000
18000
20000
20
40
60
80

Figure 4-b

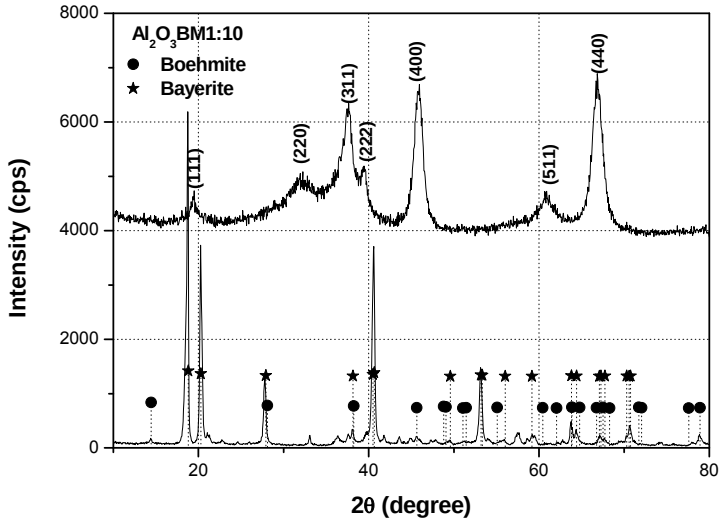
Al2O3BM1:10
Boehmite
Bayerite
(111)
(220)
(311)
(222)
(400)
(511)
(440)
Intensity (cps)
2θ (degree)
8000
6000
4000
2000
0
20
40
60
80

Figure 4-c

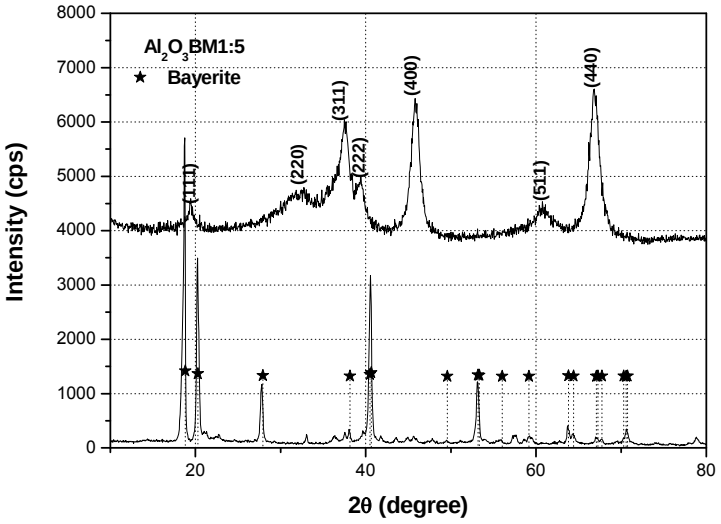
Al2O3BM1:5
Bayerite
(111)
(220)
(311)
(222)
(400)
(511)
(440)
Intensity (cps)
2θ (degree)
0
1000
2000
3000
4000
5000
6000
7000
8000
20
40
60
80

Figure 4-d

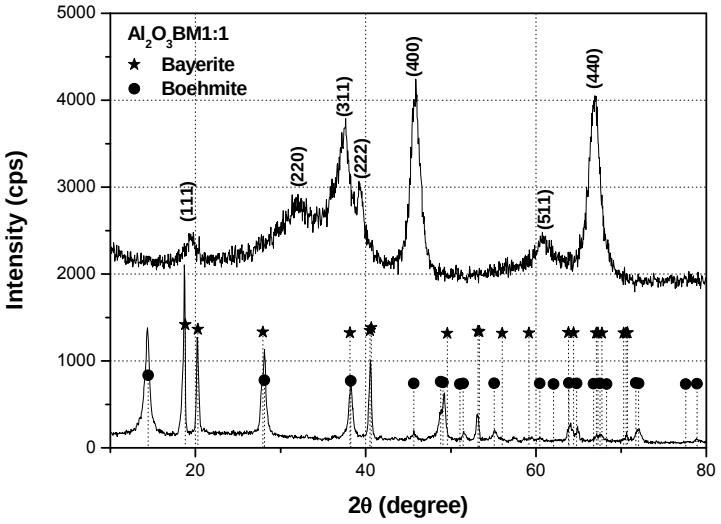
Al2O3BM1:1
Bayerite
Boehmite
(111)
(220)
(311)
(222)
(400)
(511)
(440)
Intensity (cps)
2θ (degree)
0
1000
2000
3000
4000
5000
20
40
60
80

Figure 4-e

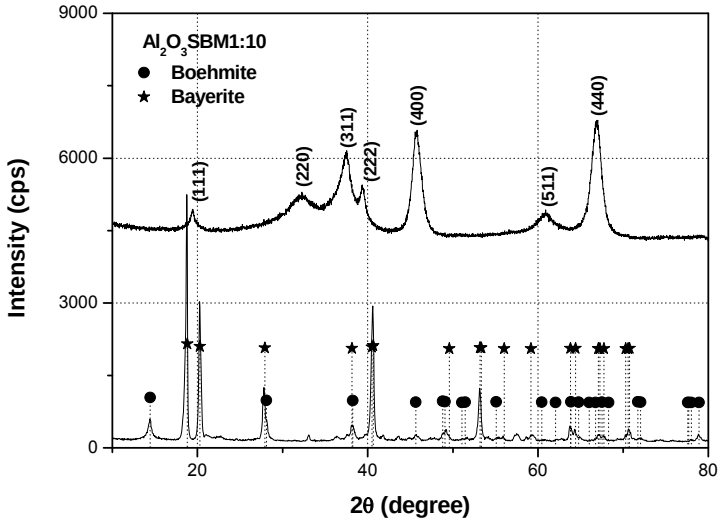
Al2O3SBM1:10
Boehmite
Bayerite
(111)
(220)
(311)
(222)
(400)
(511)
(440)
Intensity (cps)
2θ (degree)
9000
6000
3000
0
20
40
60
80

Figure 4-f

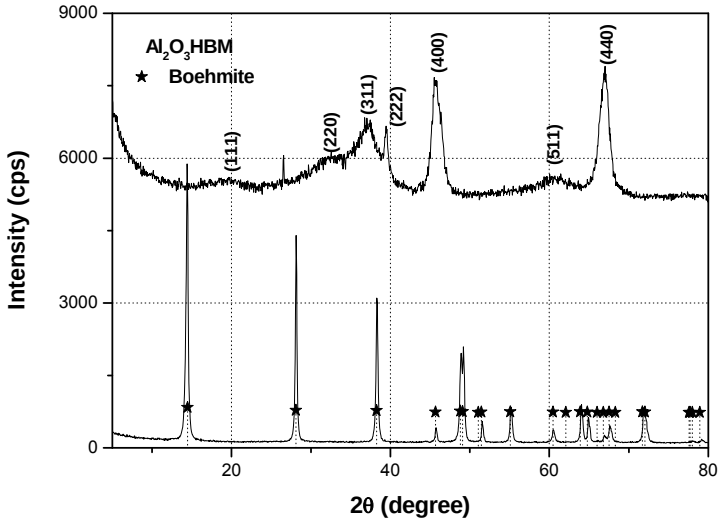
Al2O3HBM
Boehmite
(111)
(220)
(311)
(222)
(400)
(511)
(440)
Intensity (cps)
2θ (degree)
9000
6000
3000
0
20
40
60
80

Figure 4-g

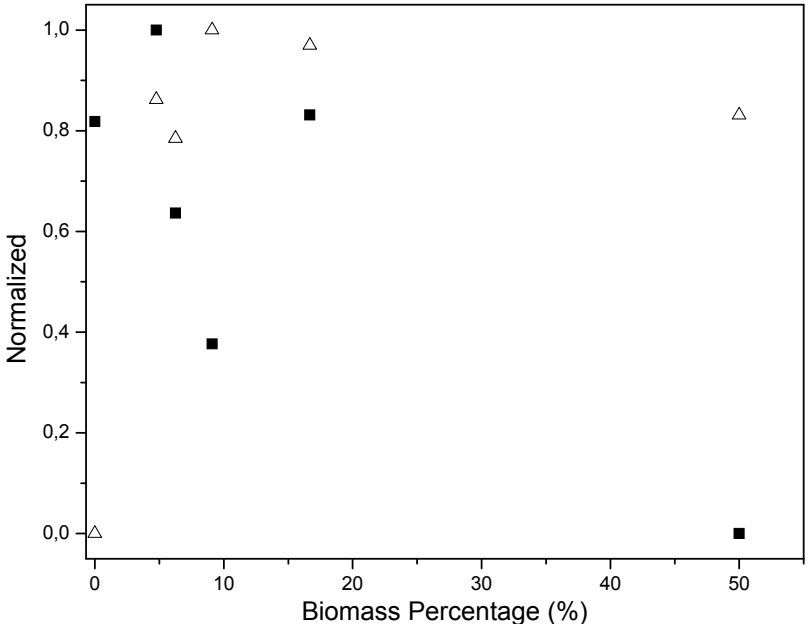

Figure 5. Normalized BET surface area (⌂) and L(111)/L(222) (■) vs biomass w**e**ight percentage.

Figure 6. HRTEM images of Al_2O_3REF1 (a,b) and Al_2O_3BM1:10 aluminas (c,d).

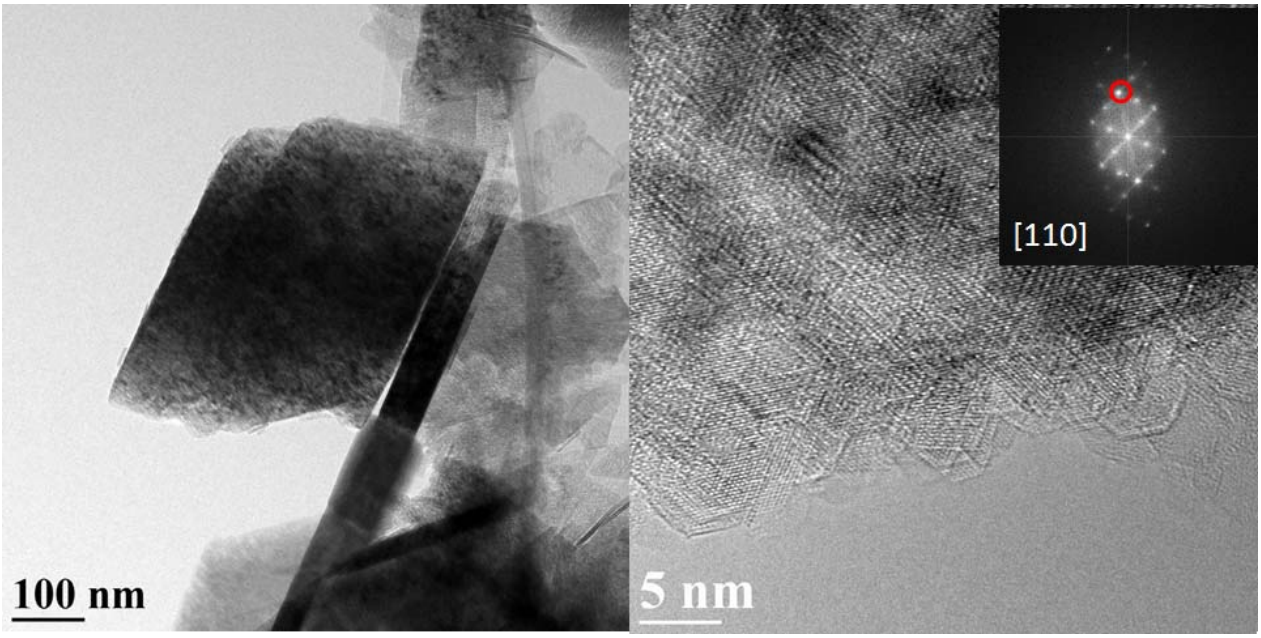

Figures 6a and 6b

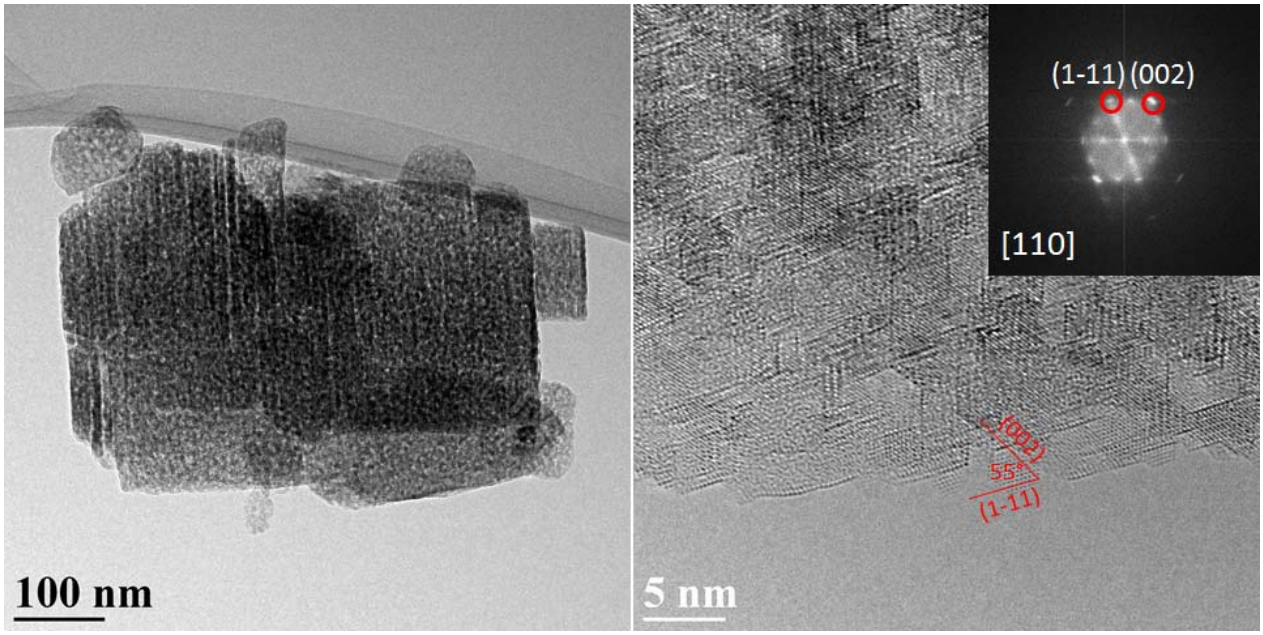

Figure 6c and d

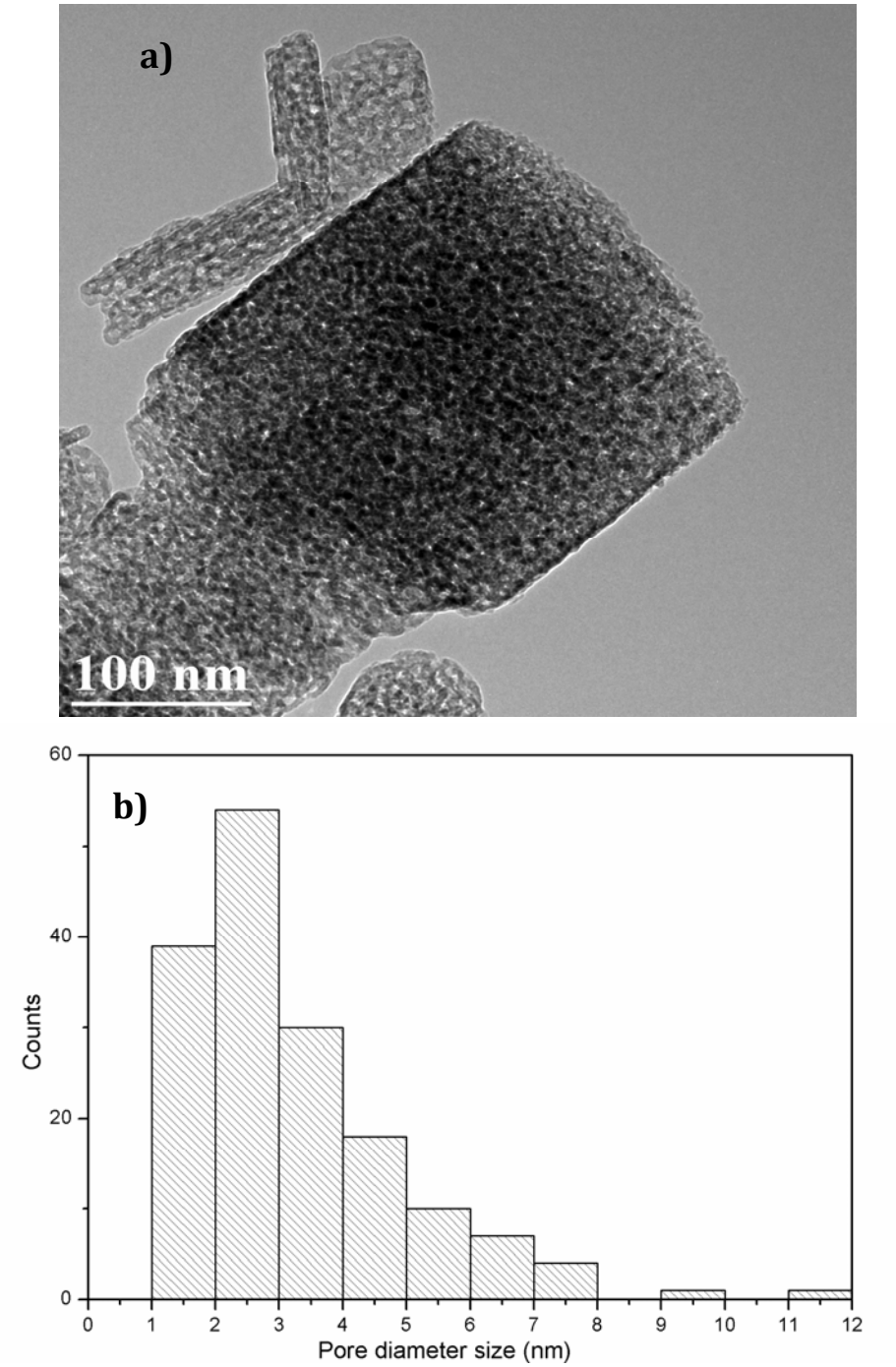

Figure 7. HRTEM image of the a) Al_2O_3 BM1:10 and b) respective distribution of diameter size of porous from HRTEM.